JMEPEG (2018) 27:3940–3950
https://doi.org/10.1007/s11665-018-3483-7

1059-9495/$19.00

Structural and Mechanical Properties of Zr-Si-N Coatings Deposited by Arc Evaporation at Different Substrate Bias Voltages

B. Warcholinski, T.A. Kuznetsova, A. Gilewicz, T.I. Zubar, V.A. Lapitskaya, S.A. Chizhik, A.I. Komarov, V.I. Komarova, A.S. Kuprin, V.D. Ovcharenko, and V.S. Goltvyanytsya

(Submitted December 15, 2017; in revised form April 26, 2018; published online July 3, 2018)

ZrN and Zr-Si-N coatings were formed using vacuum-arc plasma fluxes deposition system at the substrate bias voltage (U_B) ranged from − 50 to − 220 V on HS6-5-2 steel substrates. The structural, mechanical and tribological properties were characterized using x-ray diffraction, atomic force microscopy, scanning electron microscopy, optical microscopy, nanoindentation and ball-on-disk test. The surface roughness parameter Ra of ZrN coatings is lower than Zr-Si-N coatings. Both roughness Ra of Zr-Si-N coatings and the number of surface defects with mainly small dimensions to 1 µm decrease with increasing negative substrate bias voltage. The addition of silicon to ZrN significantly reduces the crystallite size, from about 18.3 nm for ZrN coating to 6.4 nm for Zr-Si-N coating both deposited at the same U_B = − 100 V and 7.8 nm for U_B = − 150 V. The hardness of Zr-Si-N coatings increases to about 30 GPa with the increase in negative substrate bias voltage (U_B = − 220 V). Adhesion of the coatings tested is high, and critical load is above 80 N and reduces with U_B increase. Coefficient of friction determined using AFM shows similar trend as surface roughness in microscale.

Keywords AFM, arc evaporation, grain size, microstructure, roughness Ra, Zr-Si-N

1. Introduction

The transition metal nitrides coatings are characterized by high hardness and excellent wear resistance. They are widely applied for cutting tools and tribological surfaces (Ref 1). ZrN coatings occupy a special place among them, having a favorable combination of mechanical properties under conditions requiring higher thermal stability than TiN coating (Ref 2). Addition of the third element to nitride systems improves their functional properties by changing the material behavior under the applied load. The change in mechanics behavior is realized due to structural rearrangement, when a solid substitutional solution of transition metal nitrides turns into the nanocomposite at a certain limiting concentration of particular elements (Si, C, B, etc.). The special attention is paid on silicon. In this case, nanocomposite structure consists from nanograins of cubic metal nitride (Cr, Ti, Zr) embedded in amorphous matrix of silicon nitride. It is known that the formation of an amorphous matrix in Zr-Si-N system occurs at the silicon concentration of more than 2 at.% (Ref 3). Most of the works about Zr-Si-N coatings containing silicon in an amount to about 6 at.% are focused on the microstructure and mechanical properties of the coatings (Ref 2-5). Nose et al. (Ref 5) investigated ZrN and Zr-Si-N films formed using an r.f. sputtering. They found that the hardness of the coatings with small Si concentration of about 3 at. % Si reaches the maximum value of 35 GPa. They also stated that the grain size and residual stress can make minor contributions to the hardening. Pillou et al. (Ref 6) found that hardness of the coatings with silicon concentration up to 3.5 at.% is almost constant, about 35 GPa, and linearly decreases to about 17 GPa for coatings with silicon concentration higher than about 6 at.% probably due to amorphous-like structure.

Not only the elements added to binary systems but also technological parameters, as substrate bias voltage (U_B) influences on the nanosized structure creation. The effect of U_B on the properties of Zr-Si-N coatings was rarely investigated. Song et al. (Ref 7) found that in Zr-Si-N coatings sputtered by r.f. reactive magnetron sputtering with different bias voltages the surface roughness increases as the bias voltage increases. Additionally, they stated that with the increase in negative substrate bias voltage the microstructure of Zr-Si-N coating changes from the composite that consists of nanograin ZrN and amorphous SiN_x to the composite that consists of amorphous phase. Sandu et al. (Ref 8) found that Zr-Si-N coating with 5 at.% of Si deposited at substrate bias voltage of − 150 V shows higher hardness than coating deposited at U_B = 0 V independent on deposition temperature.

Increase in negative substrate bias voltage leads to the increase in ions number bombarding the surface of the coating, and thus, to increase in plasma density. It ought to decrease in the grain size in the coatings, grain boundaries in the coating, increase in the compressive residual stresses and increasing point defects number. It promotes the increase in the coatings' microhardness.

B. Warcholinski and **A. Gilewicz**, Koszalin University of Technology, Koszalin, Poland; **T.A. Kuznetsova, T.I. Zubar, V.A. Lapitskaya,** and **S.A. Chizhik**, A.V.Luikov Heat and Mass Transfer Institute of NAS Belarus, Minsk, Belarus; **A.I. Komarov** and **V.I. Komarova**, Joint Institute of Mechanical Engineering of NAS Belarus, Minsk, Belarus; **A.S. Kuprin** and **V.D. Ovcharenko**, NSC Kharkov Institute Physics & Technology NASU, Kharkiv, Ukraine; and **V.S. Goltvyanytsya**, LLC "Real", Zaporozhye, Ukraine. Contact e-mail: bogdan.warcholinski@tu.koszalin.pl.

Unfortunately, according to our best knowledge, the systematic investigations of an effect of substrate bias voltage on Zr-Si-N coating properties were not performed. This is particularly important in the case of the mutual movement of bodies without damaging the surface layers. The high tribological properties of thin coatings are determined by their surface properties. So the study of the effect of substrate bias voltage on the microstructure and tribological properties of the Zr-Si-N coating surface is a significant problem. The standard testing methods often destruct thin coatings because of deflection of steel substrates, cracking of coating and scratching the coating by debris particles (Ref 9). Atomic force microscopy (AFM) is the technique to simultaneously study the different surface phenomena, like roughness and friction (Ref 10-12).

The aim of the work is the assessment of the effect of substrate bias voltage on surface morphology and structure characteristics of Zr-Si-N like phase composition, grain size, roughness in macro- and microscale, macroparticle statistics.

1.1 Experimental Details

A set of ZrN and Zr-Si-N coatings was formed using unfiltered cathodic arc evaporation (CAE) in a "Bulat-3T" system equipped with a Zr (99.9%) and Zr-(6 wt.%)Si cathodes of 60 mm diameter.

Zr-(6 wt.%)Si cathode was prepared by vacuum-arc melting in argon atmosphere from pure Zr (99.9%) and Si (99.9%) powders. A vacuum-arc plasma source with magnetic stabilization of a cathode spot was used. The substrates were mounted on a planetary rotating holder with a rotation speed of about 30 rpm. The substrate-cathode distance was about 300 mm. In the first step of coating deposition, the chamber was evacuated to a pressure of 2×10^{-3} Pa. Substrates were ion etched with zirconium ion bombardment by applying a DC bias of − 1300 V for 3 min. The arc current was 70 A. The second step was the improvement in the adhesion of the coatings. A pure zirconium layer (about 0.1 μm thick) was deposited on the substrate at the bias voltage of − 100 V for 3 min. The third step was deposition of the coatings. ZrN and Zr-Si-N coatings were deposited at nitrogen pressure of 2 Pa and substrate temperature 450 °C. Deposition was performed at different substrate bias voltages: − 50, − 100, − 150, − 220 V. The deposition time was 30 min in all cases and produced coatings with the thickness of about 3 μm.

X-ray diffraction (DRON-3 M, Cu Kα, 40 kV, 40 mA) was used to characterize the phase composition of the coatings. The analyzed diffraction angle (2θ) ranges from 26° to 80° with a steep of 0.05°.

A Mitutoyo profilometer was applied to determine the roughness of the coatings. The test was performed five times for one sample. To estimate the number of surface defects (macroparticles, craters) on the coatings, a Nikon Eclipse Imaging MA200 equipped with software (Imaging Software NIS-Elements) was used. The software of the microscope acquires automatically the data for the quantitative and dimensional analysis of macroparticles. The coating evaluation was carried out in the same sharpness, contrast, threshold of sensitivity, magnification (400×). The scan area was about 430×330 μm^2. The measurements were taken for each sample at five points, located in a line at equal distances from each other.

The surface morphology of Zr-Si-N coatings was investigated using atomic force microscopy (AFM) device HT-206 (produced by MTM Belarus). AFM is the technique to simultaneously study the different surface phenomena, like roughness and friction (Ref 9-12). The surface topography was studied using standard CSC38 silicon probe of beam type with the radius of tip curvature less than 10 nm and stiffness of cantilever 0.08 N/m produced by "Mikromasch" (Estonia). The roughness of the surface in microscale was investigated in fields of 2×2 μm^2. The force and coefficient of friction in microlevel were determined with AFM using 20×20 μm scanning areas with silicon probe NSC11 of V-shaped type with stiffness of cantilever 3 N/m, the radius of tip curvature about 100 nm at the speed 17 μm/s relative to the surface. The coefficient of friction is calculated from a ratio of the force of friction between two bodies and the normal force pressing them together, and their measurement is described in Ref 9.

Nano Indenter G200 system (Agilent Technologies, USA) equipped with Berkovich diamond tip was applied to determine the hardness and elastic modulus of the coatings. Ten indentations were made on each sample. The maximum load was about 30 mN. The depth of indentation was approximately 300 nm, i.e., about 0.1 of coating thickness.

The adhesion was assessed by using Revetest scratch tester (CSEM, Switzerland) equipped with diamond indenter Rockwell type C with a tip radius of 200 μm. The indenter was moved with a sliding speed of 10 mm/min. Simultaneously normal force increased linearly from 0 to 100 (150) N. Lc_2 critical force was defined as the force at which the total delamination of the coating from the substrate was observed using an optical microscope. Lc_2 is shown as the mean of at least three measurements.

Friction coefficient in macrolevel and wear rate were measured in the ball-on-disk system applying the load 20 N at 0.2 m/s of sliding speed and sliding distance from 500 to 2000 m. As a counterpart an alumina ball with 10 mm in diameter and roughness $R_a < 0.03$ μm was used. The dry condition measurements were taken in room air and relative humidity 50% at 20 °C. The profiles of wear tracks were determined with Mitutoyo profilometer. The wear rate was calculated from the material volume removed during the friction test divided by the product of load force and distance.

2. Results and Discussion

2.1 Surface Morphology and Macroparticle Statistics

TiN and ZrN show warm golden color and are widely applied as a decorative coatings (Ref 13). Addition of silicon to ZrN, as well as energy of ions during deposition (substrate bias voltage U_B), changes the color of the compounds, Fig. 1. One can see that Zr-Si-N coatings have different colors: dark brown, light brown, yellow and pale yellow for the substrate bias voltage of − 50 V (Fig. 1b), − 100 V (Fig. 1c), − 150 V (Fig. 1d) and − 220 V (Fig. 1d), respectively.

Variation of color in ZrN thin films prepared at high Ar flow rates with reactive DC magnetron sputtering was observed by Klumdoung et al. (Ref 14). They found that with the increase in the nitrogen flow rate from 0.5 sccm to 6 sccm, the color of the films changes from silver, through pale yellow, dark brown to dark blue. They also stated that above 2 sccm in nitrogen flow rate the coatings were amorphous. These conclusions confirm

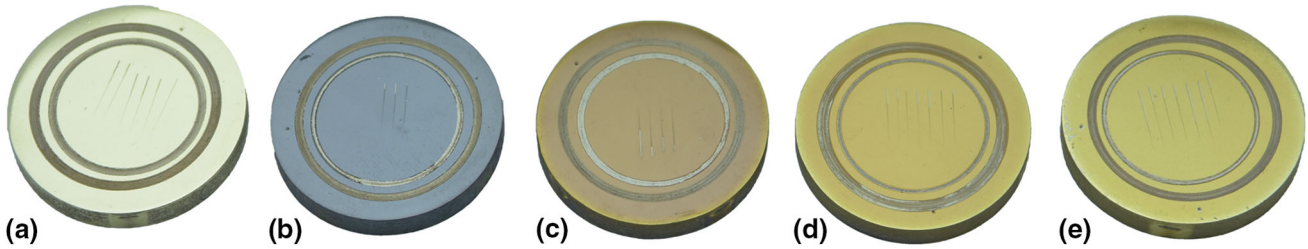

Fig. 1 The colors of ZrN coating deposited at substrate bias voltage − 100 V (a) and Zr-Si-N coatings deposited at − 50 V (b), − 100 V (c), − 150 V (d), − 220 V (e)

the investigations of Niyomsoan et al. (Ref 13) found for arc-deposited ZrN. They stated that the increase the ratio of nitrogen to zirconium causes in the overall reflectivity of the gold-like color to decrease and the yellowness to increase.

The SEM images (Fig. 2) enable the comparative microstructural characterization of ZrN and Zr-Si-N coatings deposited at different substrate bias voltages. The analysis of the macroparticles, i.e., their shapes, dimensions and number on fixed area, the surface roughness, was also performed. On the surface of all coatings the numerous macroparticles are embedded. The other types of surface defects—pores or open voids—are also observed. They all form during the deposition process, cathodic arc evaporation. The craters can be formed in different ways. The macroparticles are usually loosely bound to the coating. During deposition some of them can be removed from the surface due to ion bombardment. Other ones can be ejected because of high compressive stress in the coating related to cooling of the vacuum chamber (Ref 15). Both effects can cause a decrease in the average surface roughness R_a. It seems that higher residual stress and increased atom mobility at the bombarded surface may result in a reduction of the growth of defects with increasing bias voltage (Ref 16). The macroparticles and craters are responsible for a relatively high surface roughness of the coatings, but it seems that macroparticles have a bigger share in it.

The shape of the macroparticles is mainly spherical. They and also craters are non-uniformly distributed over the coating surface. The particle size ranges from tenths of a micrometer to several micrometers. The number of the macroparticles decreases with increasing the bias voltage, Fig. 3. Most particles are small in size—up to 1 μm independent on the type of the coating and deposition parameters. The highest number of particles was observed in the Zr-Si-N deposited at substrate bias voltage of − 50 V. For higher U_B the total number of surface defects reduces. The number of macroparticles decreases also with size. It should be noted that ZrN coating is characterized by the lowest number of surface defects in tested area. The simple correlation between number of surface defects and surface roughness was found, Fig. 4.

The number of surface defects on the coatings depends on many factors: deposition method and system, technological parameters: pressure of the reactive gas and the substrate bias voltage (Ref 17) and the type of coating (applied target) (Ref 18, 19). An increased roughness of Zr-Si-N coatings compared to ZrN coating is probably connected with a large number of macroparticles deposited on the surface. Above effect, a reduction of surface roughness of coatings as a result of an increase in substrate bias voltage was observed previously for transition metal nitride coatings: CrN (Ref 17), $WC_{0.75}N_{0.25}$ (Ref 20), Mo_2N (Ref 21).

2.2 Coatings Structure

Figure 5 shows the diffraction patterns of the ZrN deposited with a negative substrate bias voltage (− U_B) of 100 V and Zr-Si-N coatings deposited with − U_B ranged from 50 V to 220 V. The increase in negative substrate bias voltage modifies the film texture. For U_B = − 50 the intensity of (111) and (200) diffraction lines is very similar. The lines are very broad. Calculated size of the crystallites for (111) plane is about 5.2 nm, the lowest in the set of samples deposited. Intensity of the (111) peak presents the highest intensity in all coatings excluding one deposited at U_B = − 100 V.

The average size of the crystallites in ZrN calculated for (111) plane is about 18.3 nm, Table 1. Silicon addition into ZrN deposited also at the same substrate bias voltage of − 100 V results in a significant reduction in size of the crystallites to about 6.4 nm. Further increase in substrate bias voltage causes small increase in crystallite size to about 7.5 nm at U_B = − 220 V. The decrease in substrate bias voltage till U_B = − 50 V at one time with Si addition causes the further reduction of the crystallites size till 5.2 nm.

The lattice parameter of ZrN coating is slightly higher than standard one − 0.4577 nm according to PDF No 35-0753, Table 1. The Zr-Si-N coating deposited at the same technological conditions, U_B = − 100 V, shows higher lattice parameter. The results in Table 1 indicate that the higher the negative substrate bias voltage, the higher the lattice parameter.

Decrease in size of crystallites was widely described (Ref 3, 8, 22). For ZrN coatings deposited using magnetron sputtering the average size of crystallites was about 22 nm and decreases to 2.5 nm for about 10 at.% of silicon (Ref 8). Sandu et al. (Ref 8) also stated that the increase in substrate bias voltage leads to decrease in crystallite size. Similar effect was observed for TiSiN (Ref 23). Yalamanchili et al. (Ref 2) found that lattice constant of Zr-Si-N is slightly lower compared to ZrN and decreases with silicon addition increase.

It is widely known that the increase in negative substrate bias voltage causes an increase in number of ions bombarding the surface of the coating. This increases in plasma density ought to cause an decrease in the grain size in the coatings and grain boundaries in the coating. As a result, an increase in the compressive residual stresses and then the coating hardness should be observed. Really for U_B = − 100 V a significant decrease in the size of crystallites from 18.3 nm (ZrN) to 6.4 nm (Zr-Si-N) was observed. But the increase in negative substrate bias voltage for Zr-Si-N coatings results in small increase in size of crystallites, Table 1. Sandu et al. (Ref 8) found that grain size in the Zr-Si-N coatings with silicon concentration of about 3 at.%, deposited at substrate temperature 510 K and U_B = 0 V and − 150 V is about 17 nm and

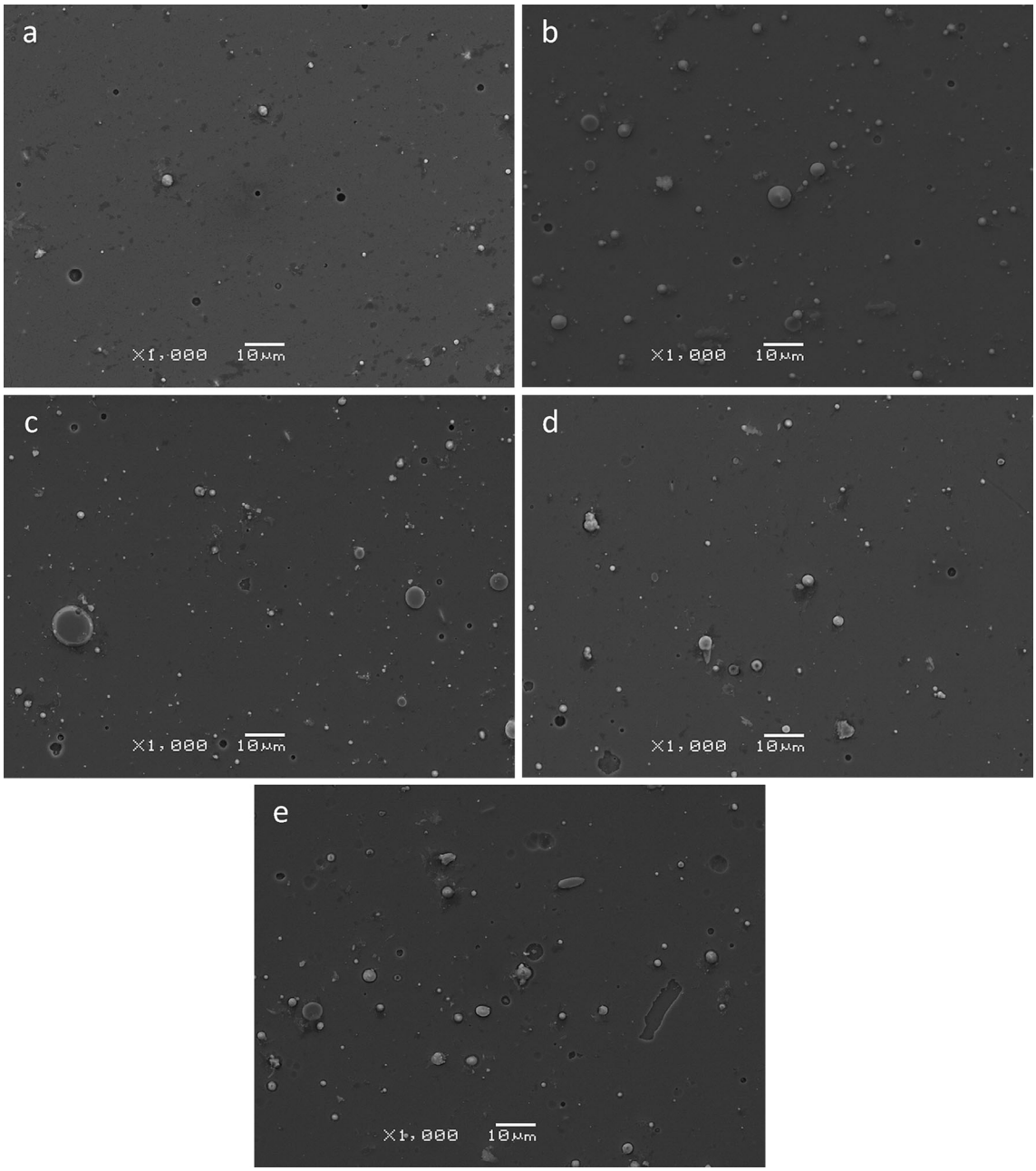

Fig. 2 Surface morphology (SEM) of ZrN coating deposited at substrate bias voltage − 100 V (a) and Zr-Si-N coatings deposited at − 50 V (b), − 100 V (c), − 150 V (d), − 220 V (e)

about 4 nm, respectively. For coatings deposited at room temperature the difference in grain size is significantly lower, 11 nm (U_B = 0 V) and 8 nm (U_B = − 150 V). The increase in silicon concentration in Zr-Si-N coating to about 5-6 at.% does not result in such large differences in grain size. The coatings deposited at room temperature show similar grain size about 6 nm. In case of the coatings deposited at temperature 510 K the grain size ranges from 6 nm (U_B = 0 V) to 4 nm (U_B = − 150 V). Investigations of Ti-Si-N coatings performed by Nose et al. (Ref 23) indicate the reduced grain size for increased substrate bias voltage.

The lattice parameter fluctuates with silicon concentration. Yalamanchili et al. (Ref 2) indicate that for small concentration of silicon the lattice parameter is higher than for ZrN coating and an increase in Si concentration above 0.6 at.% leads to reduction in lattice parameter of Zr-Si-N. Similar results but to about 4-5 at.% of silicon are presented by Sandu et al. (Ref 24). Above this silicon concentration the lattice parameter increases.

The possible explanation of the divergences is as follows. The increase in lattice parameter can be related to stress generated in deposition process during ion bombardment. The higher the negative substrate bias voltage, the higher the shift of diffraction lines toward lower angles. It is probably connected with the increase in internal stresses in the coatings.

It should be noted that the concentration of silicon and nitrogen in the coating decreases with the increase in substrate bias voltage due to the selective resputtering of light elements, silicon and nitrogen by heavy zirconium ions. The decrease in

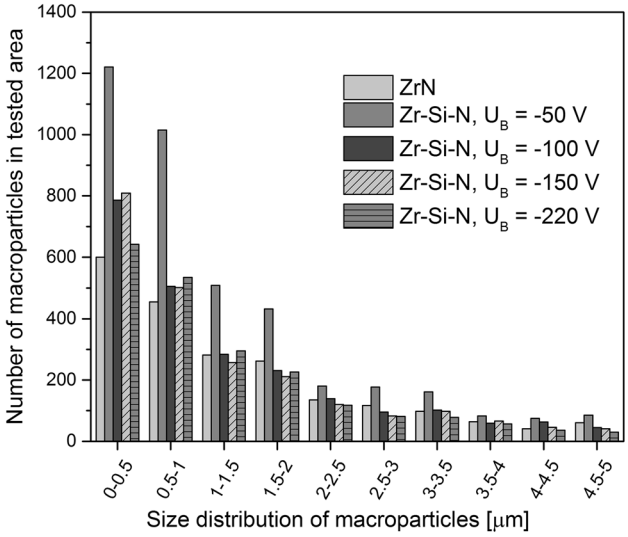

Fig. 3 Size distribution and number of macroparticles in tested area of 142049 μm^2 for ZrN and Zr-Si-N coatings deposited at different substrate bias voltage

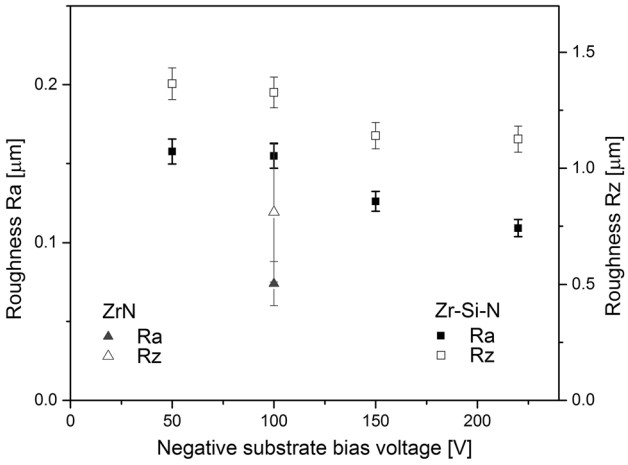

Fig. 4 The roughness Ra and Rz of ZrN and Zr-Si-N coatings deposited at different substrate bias voltage

Si concentration with the increase in substrate bias voltage can lead to the grain size increase. Above suggestions are confirmed by Sandu et al. (Ref 8) who stated that the main effect of ion bombardment during deposition of the coating is the raise of the mobility of the atoms at the surface because of increased collision of atoms.

The above divergences of the results indicate that further investigations have to be performed.

2.3 Surface Nanostructure

ZrN and Zr-Si-N coatings show classical surface microstructure characteristic for coatings deposited using PVD methods, especially cathodic arc evaporation. On the coating surface the numerous craters and a macroparticles are apparent (Fig. 6).

The amount of macroparticle phase varies within a few percent of the total area of the coating. The macroparticle phase exists in two forms: flat shape, with a surface parallel to the

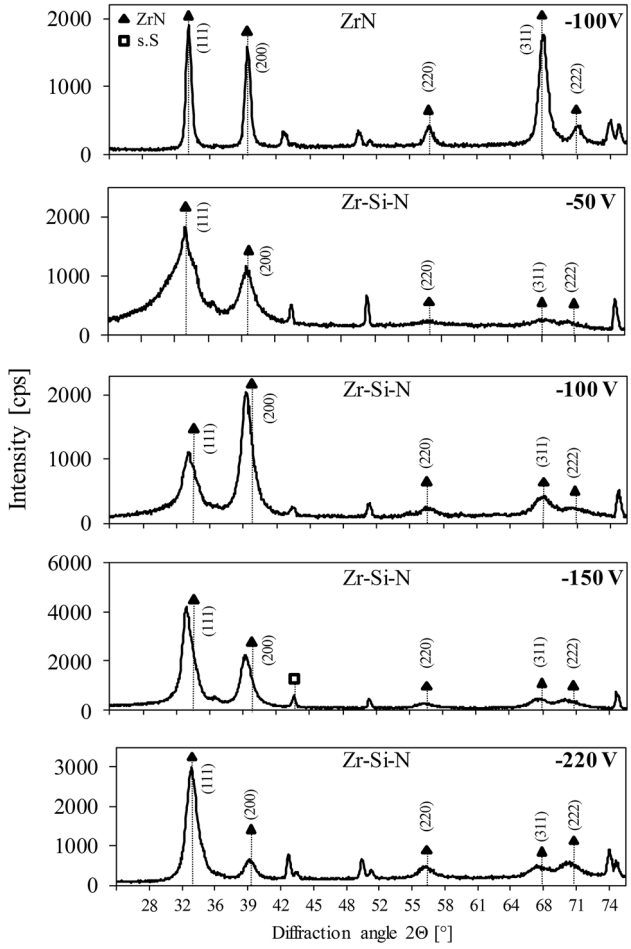

Fig. 5 X-ray diffraction patterns of ZrN and Zr-Si-N coatings deposited at different substrate bias voltages

coating (Fig. 6b), and a spherical shape (Fig. 6c). Due to the different shape of macroparticles on the surface of Zr-Si-N coatings they are probably formed from materials of different phases. Spherical macroparticles show the correct geometric shape. Around this type of macrodroplets, there are regular circles on the surface of the coating. The second type of particles has a microstructure of the surface, similar to the microstructure of the coating. Based on the view of its boundary, it seems that it has a strong mechanical connection with the coating. Intermediate forms of such particles occur in the form of "ridges" (boundaries) (Fig. 6d) or with a greater or lower amount of coating material, until a rounded island of the second coating layer is formed. Similar shapes of the macroparticles on the ZrN coatings deposited using vacuum-arc plasma fluxes at nitrogen pressures from 0.2 to 6.65 Pa were observed by Khoroshikh et al. (Ref 25). During tribological investigations using microtribometers, the macroparticles are deformed, pulled out from the coating surface and can participate in the friction process as so-called a third body.

The surface microstructure is one of the most important parameters of the coatings. The surface obtained by AFM as 3D images is interpreted as a multi-cell structure in which lowered bottom of the cells (core grain) and elevated vertical grain boundaries are visible (Fig. 7). It looks similar to Mo-C-N

Table 1 Zr-Si-N coating structural properties

Coating	Substrate bias voltage, V	Lattice parameter, nm	Crystallite size, nm
ZrN	− 100	0.4595(a)	18.3 ± 3.0
Zr-Si-N	− 50	0.4599	5.2 ± 1.3
Zr-Si-N	− 100	0.4614	6.4 ± 0.2
Zr-Si-N	− 150	0.4618	7.8 ± 0.5
Zr-Si-N	− 220	0.4637	7.5 ± 0.6

(a) According to PDF No 35-0753 for ZrN (ASTM), a = 0.4577 nm

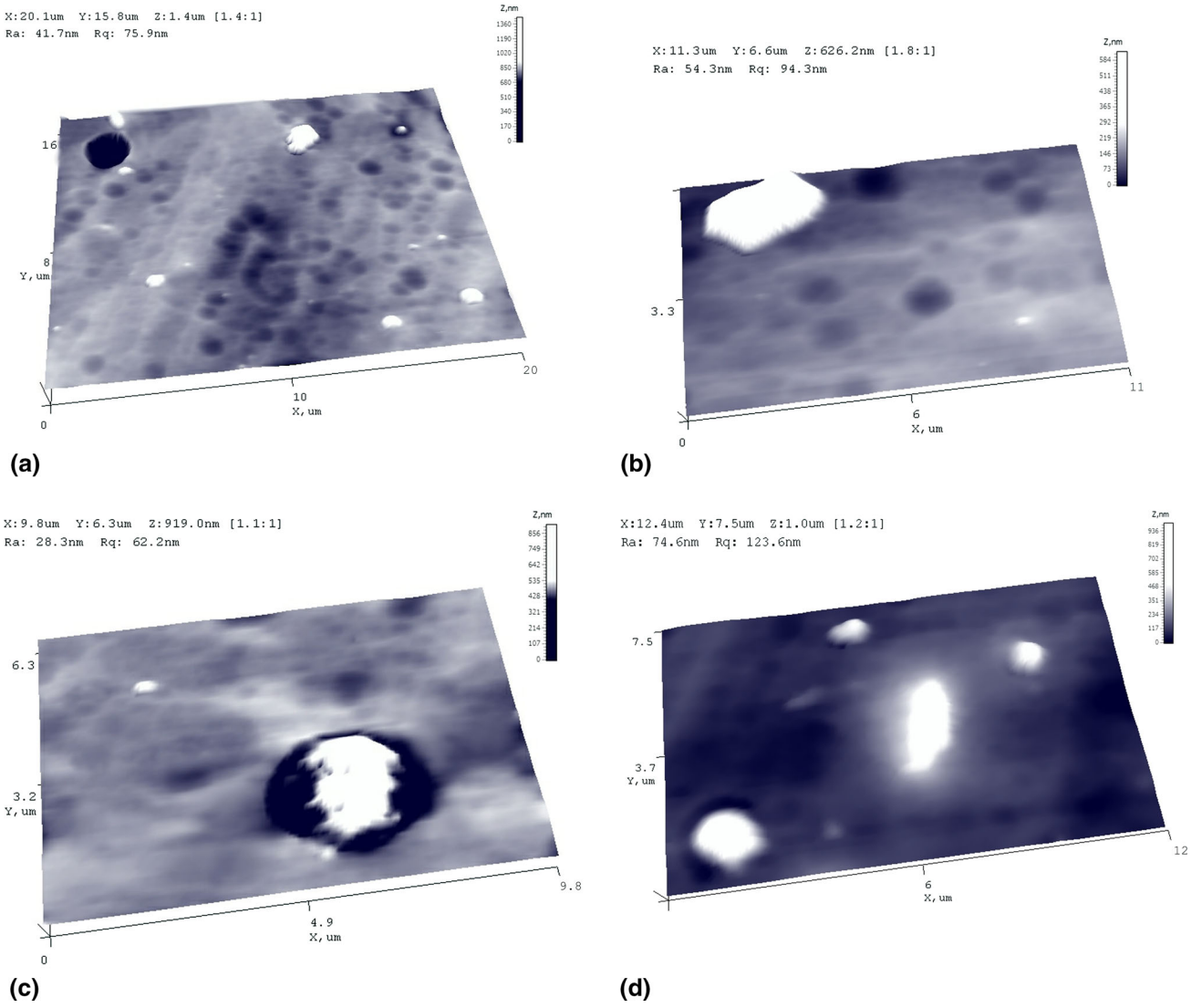

Fig. 6 AFM microstructure Zr-Si-N coatings deposited at $U_B = -150$ V with typical features: (a) scanning area 20 × 16 μm^2, (b) scanning area 11 × 7 μm^2, (c) scanning area 10 × 6 μm^2, (d) scanning area 12 × 7 μm^2

coatings which also have the third element, carbon, in nitride composition, but here the cells size is lower (Ref 26).

The significant difference in coatings microstructure is found between ZrN and Zr-Si-N coatings deposited at substrate bias voltage of -50 V and -100 V. Straight faces and edges are characteristic for ZrN coating (Fig. 7a). In Zr-Si-N coating deposited at $U_B = -50$ V the microstructure is significantly refined (Fig. 7b). The coating microstructure of Zr-Si-N deposited at $U_B = -100$ V shows the form of concave cells (Fig. 7c). The other coatings have the microstructure like

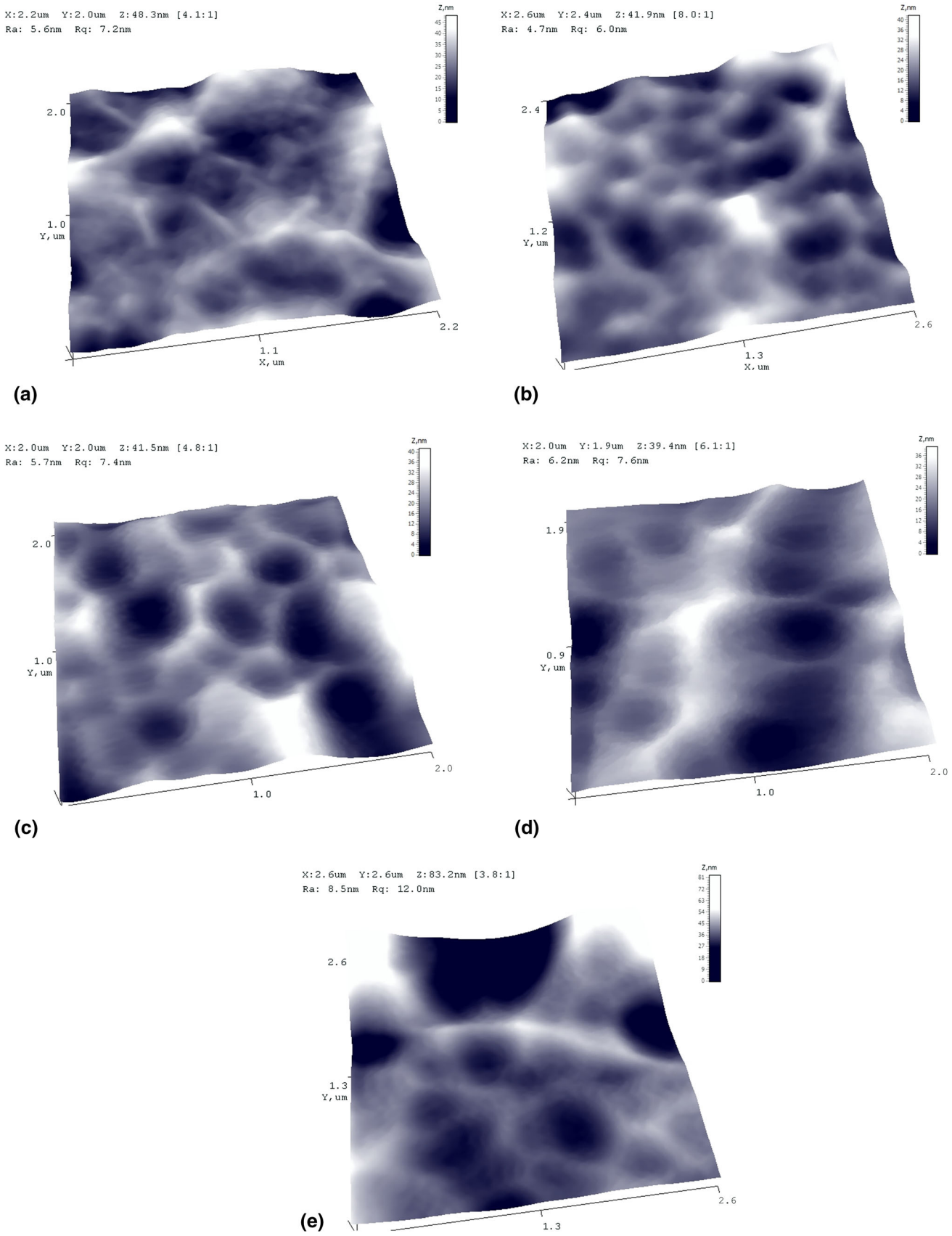

Fig. 7 AFM microstructure of ZrN coating deposited at substrate bias voltage − 100 V (a) and Zr-Si-N coatings deposited at − 50 V (b), − 100 V (c), − 150 V (d), − 220 V (e). Scanning area 2 × 2 μm^2

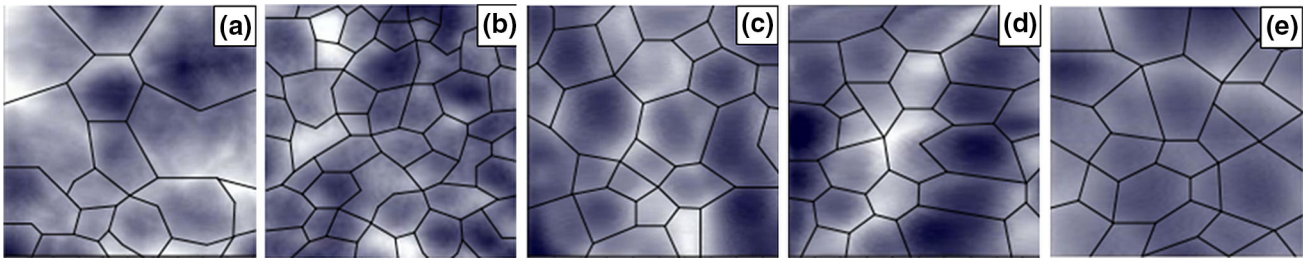

Fig. 8 The scheme of grain boundaries on the AFM microstructure with size 2 × 2 μm^2 of ZrN (a) and Zr-Si-N coatings deposited at different negative substrate bias voltage: (b) 50 V, (c) 100 V, (d) 150 V, (e) 220 V

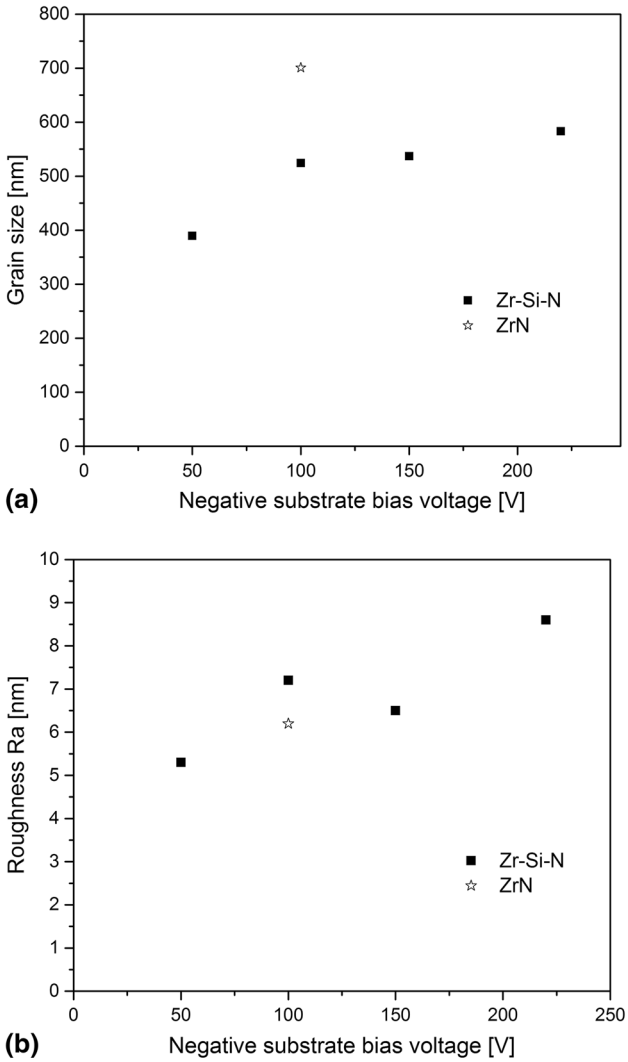

Fig. 9 Dependence of substrate bias voltage of Zr-Si-N coatings on: (a) surface grain size, (b) roughness

previous. They differ only by grain (cells) size. For the calculation of cells size the 2D microstructure was outlined in accordance with the most prominent boundaries of cells. The result of this approximation is shown in Fig. 8, and the result of grain size calculation is presented in Fig. 9(a). The reduction of the average size of the crystallites on the surface in Zr-Si-N coatings compared to ZrN coating is observed. Additionally, one can state that the higher the negative substrate bias voltage, the higher the average size of the grains. These grains which can be observed by AFM on the surface according to their white boundaries consist from small subgrains (crystallites), which can be calculated according to x-ray diffraction pattern. The increase in such grains with the increase in substrate bias voltage can be explained by the increase in zirconium ions on the surface.

The surface roughness investigations of the set of Zr-Si-N samples on the scanning area 2 × 2 μm^2 indicate that with the increase in substrate bias the roughness increases, Fig. 9(b). Above results seem to correlate with crystallite size (Table 1) calculated from XRD data.

2.4 Mechanical Properties

The hardness (H) and elastic modulus (E) of the coatings were determined from the loading–unloading curve during nanoindentation using a maximum load of 30 mN. It corresponds to a penetration depth less than 10% of the thickness of the coating. H and E values are gathered in Table 2. The hardness and elastic modulus of ZrN coating are about 28 and 400 GPa, respectively. Addition of silicon reduces both hardness and Young's modulus to about 26 and 300 GPa, respectively. The nanohardness and Young's modulus increased monotonically with the increase in negative substrate bias voltage from about 18 and 254 GPa for coatings deposited at $U_B = -50$ V, respectively, to about 30.4 and 321 GPa for $U_B = -220$ V, respectively.

The increase in hardness with negative substrate bias voltage is obvious. Due to more energetic ion bombardment the poor bonded macroparticles on the surface are removed. The surface is more smooth, the coating is denser, and the hardness increases. The values of hardness are in the hardness range for this coating and deposition method. Choi et al. (Ref 3) found the hardness and Young's modulus of ZrN deposited using hybrid coating system combining arc ion plating and DC magnetron sputtering techniques as 18 GPa and 185 GPa, respectively. The hardness and Young's modulus of ZrN deposited using reactive cathodic arc deposition technique are significantly higher, about 33 GPa and 420 GPa, respectively (Ref 2). It is known that mechanical properties of the coatings deposited using cathodic arc evaporation are better compared with magnetron sputtering. Such coatings show also higher density. It can explain higher H and E in coatings in this research. The significant decrease in hardness and Young's modulus for $U_B = -50$ V can be connected with the grain size dimension. The grain size refinement is connected with the addition of silicon to ZrN. The correlation between the hardness and the grain size of ZrN thin coatings can be formulated by the

Table 2 Results from hardness and scratch tests of Zr-Si-N coatings

Coating	Substrate bias voltage, V	Hardness, GPa	Elastic modulus, GPa	H/E	H^3/E^2	Lc_2, N
ZrN	− 100	28.0 ± 2	400 ± 10	0.070	0.137	100 ± 7
Zr-Si-N	− 50	18.0 ± 0.8	254 ± 30	0.071	0.090	108 ± 9
Zr-Si-N	− 100	25.6 ± 0.5	298 ± 3	0.086	0.189	94 ± 17
Zr-Si-N	− 150	26.6 ± 1.2	310 ± 7	0.086	0.196	82 ± 10
Zr-Si-N	− 220	30.4 ± 0.5	321 ± 6.5	0.095	0.273	79 ± 5

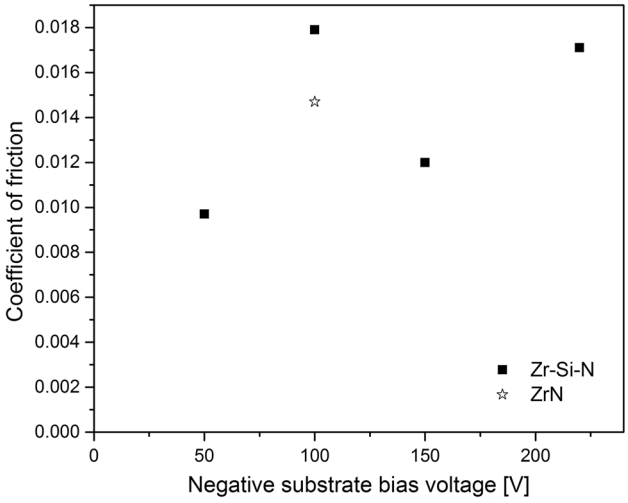

Fig. 10 Coefficient of friction of Zr-Si-N coatings deposited at different substrate bias voltage

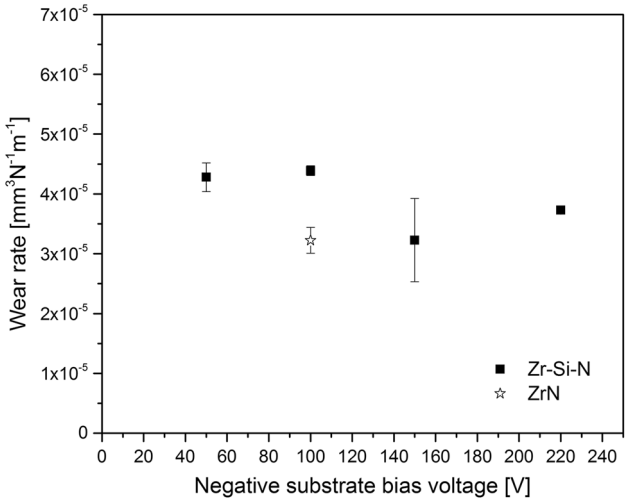

Fig. 11 The specific wear rate of Zr-Si-N coatings as a function of negative substrate bias voltage

Hall–Petch relation. The coatings Zr-Si-N deposited at U_B = − 50 nm are characterized by the smallest grain size, about 5.2 nm. With the increase in the grain size (Table 1) the hardness also increases. It can be joined with inverse Hall–Petch relation, and the hardness increases with the increase in grain size (Ref 27). Sandu et al. (Ref 8) found that maximum hardness of Zr-Si-N coatings depends on deposition temperature and substrate bias voltage. Increase in deposition temperature from RT to 510 K moves the maximum hardness from about 20 GPa to about 32 GPa for crystallite size dimensions of about 7 nm and 13 nm, respectively. Increase in negative substrate bias voltage from 0 to 150 V moves the maximum hardness from about 32 GPa to about 40 GPa for about 13 and 8 nm, respectively. The latter case is for coatings deposited at substrate temperature of 510 K. Mae et al. (Ref 22) concluded that hardness of ZrN and Zr-Si-N coating with 5.6 at.% of Si is similar, about 24-26 GPa. Both coatings are characterized by grain size of 25-35 nm. Shah et al. (Ref 28) found that maximum hardness of Cr-Si-N coating is for grain size of about 30 nm.

Based on the above results of H and E, deformation relative to yielding (H/E) and resistance to the plastic indentation (H^3/E^2) (Ref 29, 30) ratios were calculated to assess the coatings relevance for tribological applications, Table 2. Due to the increase in hardness with negative substrate bias voltage and not so high E for Zr-Si-N coating both indexes increase for Zr-Si-N coating with negative substrate bias voltage and are higher than for ZrN.

The adhesion of the coatings is one of the most important parameters affecting on its application. The coatings show high adhesion, Table 2. It decreases with negative substrate bias voltage increasing from about 108 N to about 79 N. ZrN coating is characterized by higher critical load Lc_2 compared to Zr-Si-N coating, both deposited at the same bias. Similar effect was observed by Oden et al. (Ref 31) for CrN coatings. The critical load for both cohesive failure Lc_1 and first exposure of substrate Lc_2, in a scratch test, decreased monotonically from 88 to 129 N (U_B = 20 V), respectively, with increasing negative substrate bias to 56 N and 107 N (U_B = 400 V), respectively.

Tribological properties of hard coatings depend on many factors: hardness of the coating and counterpart, roughness of the coating and counterpart, normal load, sliding speed, temperature and humidity during test, etc. The coefficient of friction of coatings tested, calculated from AFM test, is shown in Fig. 10. The values of coefficient of friction are very low. It is the lowest, about 0.01 for Zr-Si-N coating deposited at U_B = − 50 V, and the highest, about 0.018 for coating deposited at U_B = − 100 V. It should remember, that these results were obtained in AFM tests when the load is about μN and only surface layer is involved in friction process without of macroparticles destruction. On this level the roughness significantly influences on friction coefficient. It should be noted that surface roughness tested by AFM (Fig. 9b) shows similar trend. ZrN coating shows in both cases the lower values compared to Zr-Si-N coating deposited at the same substrate bias voltage.

The findings of Leyland and Matthews (Ref 29) indicate that for brittle ceramic coatings H/E ratio can give information about the tribological properties of the coatings. The optimum value of H/E is close to 0.1. For tested here Zr-Si-N coatings H/E ratio ranges from 0.07 to 0.095. The wear tests can confirm

the expected good tribological behavior of coatings tested. The trace of wear is visible in Fig. 1 in the form of circular track of abrasion. The wear rate was calculated by dividing the wear volume by the normal load and the sliding distance. The wear rates of Zr-Si-N coatings, recorded at RT and a normal load of 20 N (Hertzian contact stress about 1.3 GPa), are presented in Fig. 11. The coefficient of friction for all coatings ranges from 0.65 to 0.72. It is difficult to notice a trend of changes in the value of the wear rate. However, it is possible to point to similar changes in roughness in microscale (Fig. 9) and the coefficient of friction in the microscale (Fig. 10).

Slightly lower values of wear rate, from about 7×10^{-6} mm^3/Nm to about 14×10^{-6} mm^3/Nm, dependent on silicon concentration in the coatings were found by Yalamanchili et al. (Ref 32). They conducted the wear test under load of 5 N and the sliding distance of 100 N in ball-on-disk reciprocating-sliding system.

Pilloud et al. (Ref 33) show the wear rates based on the results of the sliding tests against 5 mm in diameter of alumina. The applied load was 25 N, sliding speed 0.005 m/s and the distance − 100 m. The wear rate decreases with the increase in silicon concentration in the coatings from 5×10^{-5} mm^3/Nm for ZrN 0 to 3×10^{-5} mm^3/Nm for Zr-Si-N coating with 4.9 at.% Si. It seems quite similar to results here presented.

3. Conclusions

ZrN and Zr-Si-N coatings formed using vacuum-arc plasma fluxes at different substrate bias voltages were investigated. The analysis of the results of the phase composition and surface morphology suggests as follows:

1. The phase composition of the Zr-Si-N coatings indicates a cubic ZrN structure with a significant shift and altered texture.
2. The lattice parameter of ZrN coating is lower compared to Zr-Si-N coatings.
3. Addition of silicon to ZrN reduces significantly the grain size of the coatings. Increase in negative substrate bias voltage results in decrease in surface roughness (macroeffect) and increase in crystalline size.
4. AFM investigations indicate that crystallite size (microeffect) and surface roughness increase with the increase in the negative substrate bias Zr-Si-N voltage during deposition.
5. The XRD and AFM results of crystallite size are totally convergent.
6. The hardness of Zr-Si-N coatings increases with the increase in negative substrate bias voltage.
7. Coefficient of friction determined using AFM shows similar trend as surface roughness in microscale.
8. According to the complex of parameters H, E, H/E, H^3/E^2, friction coefficient and wear ratio Zr-Si-N coatings can be very attractive for tribological application.
9. Adhesion of the coatings tested is high, above 80 N, what is promising in case of possible applications.

Acknowledgments

The authors would like to thank Adam Paczkowski for providing photographs of the coatings and graphics assistance.

References

1. T.A. Kuznetsova, M.A. Andreev, and L.V. Markova, Research of Wear Resistance of the Combined Vacuum Electroarc Coatings on the Basis of ZrHf, *J. Frict. Wear*, 2005, **26**(5), p 521–529
2. K. Yalamanchili, K.R. Forsén, E. Jiménez-Piqué, M.P. Johansson Jöesaar, J.J. Roa, N. Ghafoor, and M. Odén, Structure, Deformation and Fracture of Arc Evaporated Zr-Si-N Hard Films, *Surf. Coat. Technol.*, 2014, **258**, p 1100–1107
3. H. Choi, J. Jang, T. Zhang, J.H. Kim, I.W. Park, and K.H. Kim, Effect of Si Addition on the Microstructure, Mechanical Properties and Tribological Properties of Zr-Si-N Nanocomposite Coatings Deposited by a Hybrid Coating System, *Surf. Coat. Technol.*, 2014, **259**, p 707–713
4. C.S. Sandu, R. Sanjinés, and F. Medjani, Control of Morphology (ZrN Crystallite Size and SiNx Layer Thickness) in Zr-Si-N Nanocomposite Thin Films, *Surf. Coat. Technol.*, 2008, **202**, p 2278–2281
5. M. Nose, W.A. Chiou, M. Zhou, T. Mae, and M. Meshii, Microstructure and Mechanical Properties of Zr-Si-N Films Prepared by Rf-reactive Sputtering, *J. Vac. Sci. Technol. A*, 2002, **20**, p 823–828
6. D. Pilloud, J.F. Pierson, A.P. Marques, and A. Cavaleiro, Structural Changes in Zr-Si-N Films vs. Their Silicon Content, *Surf. Coat. Technol.*, 2004, **180–181**, p 352–356
7. Z. Song, K. Xu, C. Liu, The Effect of Sputtering Bias on the Composition and Microstructure of ZrSiN Diffusion Barrier Films, *IVESC2004—5th International Vacuum Electron Sources Conference Proceedings* (Beijing, China), 2004, pp. 334–336
8. C.S. Sandu, N. Cusnir, D. Oezer, R. Sanjinés, and J. Patscheider, Influence of Bias Voltage on the Microstructure and Physical Properties of Magnetron Sputtered Zr-Si-N Nanocomposite Thin Films, *Surf. Coat. Technol.*, 2009, **204**, p 969–972
9. B. Warcholinski, A. Gilewicz, T.A. Kuznetsova, T.I. Zubar, S.A. Chizhik, S.O. Abetkovskaia, and V.A. Lapitskaya, Mechanical Properties of Mo(C)N Coatings Deposited Using Cathodic Arc Evaporation, *Surf. Coat. Technol.*, 2017, **319**, p 117–128
10. S.A. Chizhik, Z. Rymuza, V.V. Chikunov, T.A. Kuznetsova, D. Jarzabek, Micro- and nanoscale testing of tribomechanical properties of surfaces, *Recent Advances in Mechatronics*, R. Jablonski et al., Ed., Springer, Leipzig, 2007, p 541–545
11. M. Andreyev, V. Anishchik, L. Markova, and T. Kuznetsova, Ion-Beam Coatings Based on Ni and Cr with Ultradispersed Diamonds—Structure and Properties, *Vacuum*, 2005, **78**, p 451–454
12. T.A. Kuznetsova, M.A. Andreev, L.V. Markova, and V.A. Chekan, Wear Resistance of Composite Chrome Coatings With Additives of Utlradispersed Diamonds, *J. Frict. Wear*, 2001, **22**(4), p 423–428
13. S. Niyomsoan, W. Grant, D.L. Olson, and B. Mishra, Variation of Color in Titanium and Zirconium Nitride Decorative Thin Films, *Thin Solid Films*, 2002, **415**, p 187–194
14. P. Klumdoung, A. Buranawong, S. Chaiyakun, and P. Limsuwan, Variation of Color in Zirconium Nitride Thin Films Prepared at High Ar Flow Rates With Reactive dc Magnetron Sputtering, *Procedia Engineering*, 2012, **32**, p 916–921
15. P. Panjan, M. Cekada, M. Panjan, and D. Kek-Merl, Growth Defects in PVD Hard Coatings, *Vacuum*, 2010, **84**, p 209–214
16. D.B. Lewis, S.J. Creasey, C. Wüstefeld, A.P. Ehiasarian, and PEh Hovsepian, The Role of the Growth Defects on the Corrosion Resistance of CrN/NbN Superlattice Coatings Deposited at Low Temperatures, *Thin Solid Films*, 2006, **503**, p 143
17. X.S. Wan, S.S. Zhao, Y. Yang, J. Gong, and C. Sun, Effects of Nitrogen Pressure and Pulse Bias Voltage on the Properties of Cr–N Coatings Deposited by Arc Ion Plating, *Surf. Coat. Technol.*, 2010, **204**, p 1800–1810

18. S. Creasey, D.B. Lewis, I.J. Smith, and W.D. Munz, SEM Image Analysis of Droplet Formation During Metal Ion Etching by a Steered Arc Discharge, *Surf. Coat. Technol.*, 1997, **97**, p 163–175
19. W.D. Munz, I.J. Smith, D.B. Lewis, and S. Creasey, Droplet Formation on Steel Substrates During Cathodic Steered Arc Metal Ion Etching, *Vacuum*, 1997, **48**, p 473–481
20. Y.D. Su, C.Q. Hu, M. Wen, C. Wang, D.S. Liu, and W.T. Zheng, Effects of Bias Voltage and Annealing on the Structure and Mechanical Properties of $WC_{0.75}N_{0.25}$ Thin Films, *J. Alloys Compd.*, 2009, **486**, p 357–364
21. A. Gilewicz, B. Warcholinski, and D. Murzynski, The Properties of Molybdenum Nitride Coatings Obtained by Cathodic Arc Evaporation, *Surf. Coat. Technol.*, 2013, **236**, p 149–158
22. T. Mae, M. Nose, M. Zhou, T. Nagae, and K. Shimamura, The Effects of Si Addition on the Structure and Mechanical Properties of ZrN Thin Films Deposited by An r.f. Reactive Sputtering Method, *Surf. Coat. Technol.*, 2001, **142–144**, p 954–958
23. M. Nose, Y. Deguchi, T. Mae, E. Honbo, T. Nagae, and K. Nogi, Influence of Sputtering Conditions on the Structure and Properties of Ti–Si–N Thin Films Prepared by r.f.-Reactive Sputtering, *Surf. Coat. Technol.*, 2003, **174–175**, p 261–265
24. C.S. Sandu, F. Medjani, R. Sanjinés, A. Karimi, and F. Lévy, Structure, Morphology and Electrical Properties of Sputtered Zr-Si-N Thin Films: From Solid Solution to Nanocomposite, *Surf. Coat. Technol.*, 2006, **201**, p 4219–4223
25. V.M. Khoroshikh, S.A. Leonov, V.A. Belous, R.L. Vasilenko, I.V. Kolodiy, A.S. Kuprin, V.A. Tikhonovskiy, and G.N. Tolmacheva, Structure and Mechanical Properties of ZrN Coatings Formed by Deposition of Vacuum arc Plasma Fluxes, *Phys. Surf. Eng.*, 2014, **12**, p 45–56 (in Russian)
26. T. Kuznetsova, T. Zubar, S. Chizhik, A. Gilewicz, O. Lupicka, and B. Warcholinski, Surface Microstructure of Mo(C)N Coatings Investigated by AFM, *J. Mater. Eng. Perform.*, 2016, **25**, p 5450–5459
27. T.G. Nieh and J. Wadsworth, Hall-Petch Relation in Nanocrystalline Solids, *Scri. Metall. Mater.*, 1991, **25**, p 955–958
28. H.N. Shah, R. Jayaganthan, and D. Kaur, Influence of Silicon Content on the Microstructure and Hardness of CrN Coatings Deposited by Reactive Magnetron Sputtering, *Mater. Chem. Phys.*, 2010, **121**, p 567–571
29. A. Leyland and A. Matthews, On the Significance of the H/E Ratio In wear Control: A Nanocomposite Coating Approach to Optimized Tribological Behaviour, *Wear*, 2000, **246**, p 1–11
30. J. Musil, F. Kunc, H. Zeman, and H. Polakova, Relationships Between Hardness, Young's Modulus and Elastic Recovery in Hard Nanocomposite Coatings, *Surf. Coat. Technol.*, 2002, **54**, p 304–313
31. M. Odén, C. Ericsson, G. Håkansson, and H. Ljungcrantz, Microstructure and Mechanical Behavior of Arc-Evaporated Cr–N Coatings, *Surf. Coat. Technol.*, 1999, **114**, p 39–51
32. K. Yalamanchili, E. Jiménez-Piqué, L. Pelcastre, K.D. Bakoglidis, J.J. Roa, M.P. Johansson Jõesaar, B. Prakash, N. Ghafoor, and M. Odén, Influence of Microstructure and Mechanical Properties on the Tribological Behavior of Reactive arc Deposited Zr-Si-N Coatings at Room and High Temperature, *Surf. Coat. Technol.*, 2016, **304**, p 393–400
33. D. Pilloud, J.F. Pierson, and J. Takadoum, Structure and Tribological Properties of Reactively Sputtered Zr-Si-N Films, *Thin Solid Films*, 2006, **496**, p 445–449